

# Identifying a characterized energy level structure of higher charmonium well matched to the peak structures in $e^+e^- \rightarrow \pi^+D^0D^{*-}$

Jun-Zhang Wang<sup>1,2\*</sup> and Xiang Liu<sup>2,3,4,5†</sup>

<sup>1</sup>*School of Physics and Center of High Energy Physics, Peking University, Beijing 100871, China*

<sup>2</sup>*School of Physical Science and Technology, Lanzhou University, Lanzhou 730000, China*

<sup>3</sup>*Lanzhou Center for Theoretical Physics, Key Laboratory of Quantum Theory and Applications of MoE, Key Laboratory of Theoretical Physics of Gansu Province, Lanzhou University, Lanzhou 730000, China*

<sup>4</sup>*Moe Frontiers Science Center for Rare Isotopes, Lanzhou University, Lanzhou 730000, China*

<sup>5</sup>*Research Center for Hadron and CSR Physics, Lanzhou University & Institute of Modern Physics of CAS, Lanzhou 730000, China*

(Dated: June 27, 2023)

Recent advancements in charmoniumlike state have significantly enriched the discovery of new hadronic states, providing exciting opportunities for further investigations into the fascinating realm of charmonium physics. In this letter, we focus on the vector charmonium family and perform a detailed analysis of the recently observed  $e^+e^- \rightarrow \pi^+D^0D^{*-}$  process. Our findings demonstrate a striking agreement between the observed peak structures and the predicted characterized energy level structure of higher vector charmonia including the  $\psi(4220)$ ,  $\psi(4380)$ ,  $\psi(4415)$ , and  $\psi(4500)$ , which are derived from an unquenched potential model. This discovery challenges conventional understanding of higher charmonia above 4 GeV and offers fresh insights into the dynamics of charm and anti-charm quarks in the formation of these states. Furthermore, the identification of these higher charmonia in the precisely measured  $\pi^+D^0D^{*-}$  open-charm decay channel would serve as compelling evidence supporting the unquenched scenario and contribute to a deeper understanding of the nonperturbative aspects of the strong interaction.

*Introduction.*—As we enter the 21st century, higher precision experiments have yielded a plethora of surprising and promising results in hadron spectroscopy. Notably, a series of new hadronic states, such as the charmoniumlike  $XYZ$  and  $P_c$  states, have been discovered [1–7]. This marks the onset of a new phase of hadron spectroscopy research, which may provide valuable insights into the nonperturbative problem of the strong interaction, a long-standing puzzle in particle physics.

In the 1970s, the observation of the  $J/\psi$  particle [8, 9] introduced a new class of hadrons known as charmonium. Subsequently, experimentalists discovered numerous charmonium states, which now constitute the bulk of charmonium cataloged by the Particle Data Group (PDG) [1]. Moreover, these observations of charmonium stimulated the development of the Cornell model with the linear plus Coulomb potential, a quenched potential model proposed by Eichten *et al.* [10, 11]. This model has inspired various potential models, including famous Godfrey-Isgur (GI) model [12], which facilitates quantitative calculations of hadron spectroscopy.

Although substantial progress has been made in the field of hadron spectroscopy, it is important to note that our current understanding of it is not yet complete. In particular, establishing the energy level structure of higher charmonium states above 4.2 GeV has remained a challenge for several decades since the discovery of the  $J/\psi$ . In 2014, the Lanzhou group drew attention to the striking similarity between the charmonium and bottomonium families [13]. They determined the mass of the narrow-width charmonium state  $\psi(4S)$  to be 4263 MeV, which is markedly different from the conventional assignment of  $\psi(4415)$  as the  $\psi(4S)$  under quenched potential models such as the Cornell model [10, 11]. However, this result is consistent with the expectations from the screening potential [14, 15].

Soon after, the BESIII Collaboration surprised us with the

discovery of narrow structures around 4.2 GeV referred to as the  $Y(4220)$  in processes involving  $e^+e^-$  annihilations into hidden-charm channels, such as  $J/\psi\pi^+\pi^-$  [16],  $h_c\pi^+\pi^-$  [17],  $\omega\chi_{c0}$  [18], and  $\psi(3686)\pi^+\pi^-$  [19]. These observations were consistent with the expectation that there is a charmonium state, the  $\psi(4220)$  [20]. Taking this opportunity, researchers realized the potential of the observed  $Y(4220)$  narrow structure as a scaling point for constructing the energy level structure of higher charmonia above 4.2 GeV in Ref. [21]. By using an unquenched potential model, the  $Y(4220)$  was assigned to the charmonium family under the  $4S$ - $3D$  mixing scheme, and its charmonium partner  $\psi(4380)$  was predicted [21]. During this process, the well-established  $\psi(4415)$  was proposed as a  $5S$ - $4D$  mixing state, while its charmonium partner  $\psi(4500)$  was also found to exist [21, 22]. As a result, a characterized energy level structure for higher vector charmonia above 4.2 GeV has been obtained under an unquenched potential model. Given this research background, identifying this predicted higher charmonium energy level structure in its open-charm decay channels has become a critical step in the entire study. Open-charm decay channels are known to dominate the widths of higher charmonia, and their contributions may provide crucial evidence to test such a scenario.

In recent years, the BESIII Collaboration has made significant progress in measuring the  $e^+e^-$  annihilation processes into open-charm channels [23–27]. In this letter, it is reported that the peak structures observed in the newly observed  $e^+e^- \rightarrow \pi^+D^0D^{*-}$  process match well with the characterized energy level structure of higher vector charmonia predicted by the unquenched potential model, which includes the  $\psi(4220)$ ,  $\psi(4380)$ ,  $\psi(4415)$ , and  $\psi(4500)$  states. This finding challenges our long-held perception of higher charmonia above 4 GeV and sheds new light on how charm and anti-charm quarks interact to form these states. The identification of these key

higher charmonia in the  $\pi^+ D^0 D^{*-}$  open-charm decay channel not only provides crucial evidence to test the unquenched scenario but also enriches our understanding of the nonperturbative aspects of the strong interaction.

*The emergence of the charmonium structures with characterized energy level in  $e^+e^- \rightarrow \pi^+ D^0 D^{*-}$ .*—In recent decades, the discovery of various charmoniumlike  $XYZ$  states has brought attention to the significant role of the unquenched effect in the color confinement potential [2]. Building upon these advancements, we have directed our attention to the challenging charmoniumlike  $Y$  problem, offering a promising solution framework through the implementation of an unquenched quark potential model, as detailed in our previous work [21]. Utilizing the unquenched results, we have successfully predicted a comprehensive and distinct characterized energy spectrum for vector charmonia within the range of 4.2 to 4.6 GeV [21], which starkly contrasts the predictions derived from conventional quark models [10, 11]. To explore this characterized energy level structure, the selection of a suitable reaction process becomes a crucial concern. From a hadron-level perspective, the pronounced unquenched effect typically indicates a strong coupling between the charmonium state and its two-body open charm channels, particularly in the case of  $S$ -wave interactions [11, 28–31]. Notably, for vector charmonium, the lowest  $S$ -wave open charm channels encompass  $DD_1(2420)$ ,  $DD_1(2430)$ ,  $DD_0^*(2300)$ , and others. Remarkably, these two-body modes predominantly decay into three-body final states such as  $DD^*\pi + c.c.$ . Consequently, the  $e^+e^- \rightarrow \pi^+ D^0 D^{*-}$  process serves as a unique and valuable means to experimentally probe the behavior of higher charmonia spectra above 4 GeV.

The reaction dynamics of  $e^+e^- \rightarrow \pi^+ D^0 D^{*-}$  is dominated by two-part contributions, i.e., the direct production and intermediate charmonium contribution. The amplitude of direct production can be described by a parameterized form

$$\mathcal{A}_0 = g \left( \sqrt{s} - m_D - m_{D^*} - m_\pi \right)^2 e^{-a_0 s}. \quad (1)$$

And then the amplitude associated with intermediate charmonium can be written as

$$\mathcal{A}_i = \sqrt{12\pi R_i \Gamma_i} B(s, m_i, \Gamma_i) \sqrt{\Phi(\sqrt{s})/\Phi(m_i)} e^{i\phi_i}, \quad (2)$$

where  $B(s, m_i, \Gamma_i) = (s - m_i^2 + im_i\Gamma_i)^{-1}$  is the Breit-Wigner function, and  $m_i$ ,  $\Gamma_i$ ,  $\Phi(\sqrt{s})$  and  $\phi_i$  are the mass and width of the intermediate charmonium state, three-body phase space and phase angle, respectively. The  $R_i$  is the product of dilepton width  $\Gamma(\psi \rightarrow e^+e^-)$  and branching ratio  $\mathcal{B}(\psi \rightarrow \pi^+ D^0 D^{*-})$ . The corresponding cross section distribution against the center-of-mass energy  $\sqrt{s}$  is

$$\sigma(s) = \left| \mathcal{A}_0(s) + \sum_i \mathcal{A}_i(s) \right|^2. \quad (3)$$

We noticed that the Born cross section of  $e^+e^- \rightarrow \pi^+ D^0 D^{*-}$  between 4.05 and 4.60 GeV had been recently released by the BESIII Collaboration [23]. In their analysis, two broad

enhancements were observed in the invariant mass spectrum of  $\pi^+ D^0 D^{*-}$ , specifically around 4.2 and 4.4 GeV. However, the origin of these enhancements remains unclear at present. This presents us with an excellent opportunity to explore and identify the predicted characterized energy spectrum of higher vector charmonium. Accordingly, the information of the characterized energy level structures are summarized in Table I.

Referring to Table I, it can be known that within the experimental energy range, there are four distinct underlying charmonium structures, in addition to the well-established charmonium state  $\psi(4160)$ . The presence of multiple resonances and their interference can often lead to a serious multiple solutions problem in concrete analyses [32–34], which has to be carefully considered here. Starting from a general amplitude function in Eq. (3), it can be written as

$$\mathcal{A}(s) = \left( z_0 D(s) + \sum_{k=1}^{k=n} z_k B_k(s) \right) \Phi(\sqrt{s})^{1/2}, \quad (4)$$

where  $D(s)$  is the direct amplitude function involving the energy-dependent term and  $B_k(s) = B(s, m_k, \Gamma_k) = (s - p_k)^{-1}$  with  $p_k = m_k^2 - im_k\Gamma_k$ . If the amplitude function  $\mathcal{A}(s)$  has a series of zero points  $\{x_m\}$  after making an analytical continuation of  $s$  in the complex plane, by applying the Weierstrass factorization theorem [35], it can be factorized as

$$\mathcal{A}(s) = \prod_m (s - x_m) \mathcal{N}(s, \{z_0, z_k\}) \Phi(\sqrt{s})^{1/2}, \quad (5)$$

where  $\mathcal{N}$  function does not include any zero structures. Now our purpose is to search for a other set of solution  $\{z'_0, z'_k\}$ , which satisfies

$$\left| \prod_m (s - x_m) \mathcal{N}(s) \right| = \left| \prod_m (s - x'_m) \mathcal{N}'(s) \right| \quad (6)$$

for any  $s$  in a real range. Due to the disparate structure in Eq. (6), one can conclude that  $|(s - x_m)| = |(s - x'_m)|$  and  $|\mathcal{N}(s)| = |\mathcal{N}'(s)|$ . Here, it can be firstly known that  $x'_m = x_m$  or its complex conjugate  $x_m^*$ . Additionally, by applying the identical relation

$$B_k(s) = -(s - x_m) B_k(s) / (x_m - p_k) + B_k(x_m), \quad (7)$$

the  $\mathcal{N}(s)$  in Eq. (5) can be simplified as

$$\begin{aligned} \mathcal{N}(s, \{z_0, z_k\}) &= C(z_0, D(s), \{D(x_m)\}) \\ &+ (-1)^n \sum_{k=1}^n \frac{z_k}{\prod_m (x_m - p_k)} B_k(s). \end{aligned} \quad (8)$$

Because  $\mathcal{N}$  function has no any zeros, in which each components are linearly independent, so the equation  $|\mathcal{N}(s)| = |\mathcal{N}'(s)|$  means that

$$|C(z_0, D(s), \{D(x_m)\})| = |C(z'_0, D(s), \{D(x'_m)\})|, \quad (9)$$

$$\left| \frac{z_k}{\prod_m (x_m - p_k)} \right| = \left| \frac{z'_k}{\prod_m (x'_m - p_k)} \right|. \quad (10)$$

These two equations play a crucial role in analyzing the issue of multiple solutions caused by resonance interference. In Eq. (10), if we consider the direct continuum contribution in  $e^+e^- \rightarrow \pi^+D^0D^{*-}$  to be negligible and therefore ignored, we would anticipate obtaining 16 sets of  $\{z'_k\}$  solutions with identical fitting quality by making different replacements of  $x'_m$  with  $x_m^*$ . These solutions are nearly impossible to distinguish using various theoretical models. However, it is important to note that Eq. (9) is generally not easily satisfied by the majority of the continuum term. In the following, it can be seen that the direct continuum contribution in our fit is significant, enabling us to overcome the challenge of multiple solutions.

The unknown parameters in the cross section analysis of  $e^+e^- \rightarrow \pi^+D^0D^{*-}$  mainly include  $g$ ,  $a_0$  in the continuum amplitude and  $R_i$  and angle phase  $\phi_i$  in the charmonium amplitudes. The input of masses and widths of the intermediate charmonia can be found in Table I. The fitted cross section distribution of  $e^+e^- \rightarrow \pi^+D^0D^{*-}$  is depicted in Fig. 1, and the corresponding fitted parameters are summarized in Table II. It is evident that the experimental data can be well reproduced with clear signals of the four characterized energy level structures, as indicated by the fitted  $\chi^2/d.o.f. = 0.74$ . Notably, the BESIII's study concluded that the second high-mass enhancement cannot be explained by a single resonance and possesses a more intricate underlying structure [23]. In this regard, the characterized energy spectrum of charmonium provides a very natural explanation for this phenomenon. Specifically, the interference between the  $\psi(4415)$  and the predicted characterized structure  $\psi(4380)$  near 4.4 GeV can generate an extremely broad enhancement. Furthermore, BESIII has suggested categorizing the first enhancement as  $Y(4220)$  [23], but its measured width of  $77 \pm 6.8 \pm 6.3$  MeV [23] obviously deviates the narrow width of  $44.1 \pm 4.3 \pm 2.0$  ( $28.2 \pm 3.9 \pm 3.6$ ) MeV in hidden-charm channel  $J/\psi\pi^+\pi^- (\chi_{c0}\omega)$  [16, 18] as well as the theoretical prediction of (23 ~ 30) MeV [21] for the charmonium  $\psi(4220)$ . However, our present analysis has convincingly proved that the first enhancement can be described within a multi-resonance interference scheme, with a narrow width of  $\Gamma(\psi(4220)) = 44$  MeV as an input. As a result, this disagreement in widths can also be effectively resolved. From this perspective, we can confidently conclude that the enhancement structures observed in  $e^+e^- \rightarrow \pi^+D^0D^{*-}$  indeed match well our prediction for the characterized energy spec-

TABLE I: The information of the predicted characterized energy level structure of higher vector charmonia.

State	Assignment	Mass (MeV) [21, 22]	Width (MeV) [21, 22]
$\psi(4220)$	$\psi'_{4S-3D}$	4222	44
$\psi(4380)$	$\psi''_{4S-3D}$	4389	80
$\psi(4415)$	$\psi'_{5S-4D}$	4414	33
$\psi(4500)$	$\psi''_{5S-4D}$	4509	50

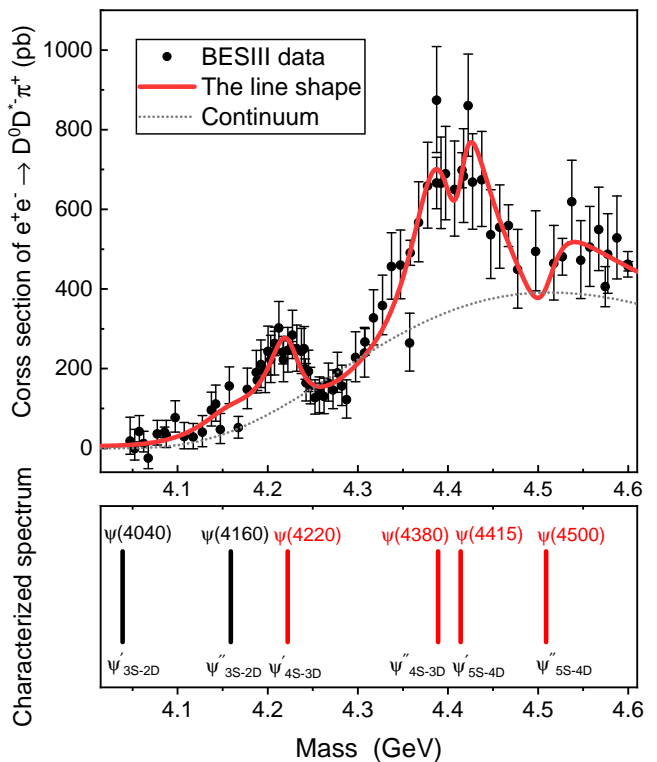


FIG. 1: The emergence of the characterized energy level structures of higher vector charmonia in the cross section distribution of  $e^+e^- \rightarrow \pi^+D^0D^{*-}$ . Here, the black lines and red lines in the bottom plot represent for the established charmonia and the predicted characterized charmonium structures in the unquenched scheme, respectively.

trum of higher vector charmonia. This alignment serves as a strong indication for unraveling the nature of several reported charmoniumlike  $Y$  states. From Fig. 1 and Table II, it can be also seen that the continuum contribution is highly significant and the only one set of solution for  $\{R_i, \phi_i\}$  has been found when adopting the background form of  $\mathcal{A}_0$  in Eq. (1). This result implies that it will be convenient to continuously identify the characterized energy level structures of charmonia by comparing the fitted  $R_i$  values with the corresponding theoretical three-body  $\pi^+D^0D^{*-}$  decay behaviors, which will be discussed in detail later.

*The three-body  $DD^*\pi$  decay behaviors of higher vector charmonia.*— In this section, our attention turns to the examination of the three-body  $\pi^+D^0D^{*-}$  decay behaviors of higher vector charmonia. The fitted  $R_i = \Gamma_{e^+e^-}^{\psi_i} \mathcal{B}(\psi_i \rightarrow \pi^+D^0D^{*-})$  directly quantifies the magnitude of the intermediate charmonium contribution. Thus, this physical quantity encodes important information for understanding the properties of higher charmonium states. Very interestingly, one can find that the magnitudes of  $R_i$  for  $i = \psi(4040)$ ,  $\psi(4220)$ ,  $\psi(4415)$  and  $\psi(4500)$  are approximately close to the range of 1.0 ~ 3.0 eV as listed in Table II, while the  $R_{\psi(4380)} = 19.0 \pm 4.6$  eV is significantly larger. For probing this phenomenon, we need to quantitatively calculate the three-body  $DD^*\pi$  decay behaviors

of higher charmonia. The decay processes of  $\psi \rightarrow D\bar{D}^*\pi + c.c.$  are generally achieved via the direct coupling and two kinds of cascade decays from intermediate charmed meson states, i.e.,  $\psi \rightarrow D\bar{D}^{***} + c.c. \rightarrow D(\bar{D}^{***} \rightarrow \bar{D}^*\pi) + c.c.$  and  $\psi \rightarrow D^*\bar{D}^{**} + c.c. \rightarrow D^*(\bar{D}^{**} \rightarrow \bar{D}\pi) + c.c.$ , where  $\bar{D}^{***}$  or  $\bar{D}^{**}$  is the allowed intermediate charmed meson state. Due to the absence of experimental information, it is hard to quantitatively discuss the direct coupling contribution. However, the two-body cascade decay contribution may be enough for us to make a rough discussion on the decay behaviors of  $\pi^+D^0D^{*-}$  because the summation for theoretical two-body OZI-allowed strong decay widths of many heavy quarkonia are already consistent with the corresponding experimental total widths [36–38]. By consulting the two-body open charm decay behaviors of the characterized energy level structures of higher vector charmonia [21] and the charmed meson family information [39], we mainly consider four intermediate charmed meson states, i.e.,  $D^{***} = D_1(2420), D_1(2430), D_2^*(2460)$  and  $D^{**} = D_0^*(2300)$ . Within the effective Lagrangian approach [40], their corresponding decay amplitudes are written as

$$\begin{aligned} \mathcal{M}_{D_0} &= \frac{g_{\psi D^* D_0} \epsilon_{\psi\mu} \epsilon_{D^*}^{*\mu}}{q'^2 - m_{D_0}^2 + im_{D_0} \Gamma_{D_0}} g_{D_0 D \pi}, \\ \mathcal{M}_{D_1} &= g_{\psi DD_1} \epsilon_{\psi\mu} \frac{-g^{\mu\nu} + q^\mu q^\nu / m_{D_1}^2}{q^2 - m_{D_1}^2 + im_{D_1} \Gamma_{D_1}} g_{D_1 D^* \pi} \epsilon_{D^*}^{*\nu}, \\ \mathcal{M}_{D_2} &= g_{\psi DD_2} \epsilon_{\rho\lambda\mu\nu} p^\mu (p - q_2)^\nu \epsilon_{\psi}^\rho (p + q_2)^\alpha g_{D_2 D^* \pi} \\ &\quad \times \frac{\mathcal{G}_{\alpha\beta}^{\lambda\tau}(q^2) \epsilon_{\kappa\tau\gamma\chi} q_3^\gamma (p - q_2)^\chi \epsilon_{D^*}^{*\kappa} (q_4 - q_3)^\beta}{q^2 - m_{D_2}^2 + im_{D_2} \Gamma_{D_2}}, \end{aligned} \quad (11)$$

where  $p, q_2, q_3, q_4$  are four-momentum of  $\psi, D, D^*, \pi$ , respectively, and  $q' = p - q_3$  and  $q = p - q_2$ . The spin projection operator of tensor particle  $\mathcal{G}_{\alpha\beta}^{\lambda\tau}(q^2) = \frac{1}{2}(\tilde{g}_\alpha^\tau \tilde{g}_\beta^\lambda + \tilde{g}_{\alpha\beta} \tilde{g}^{\tau\lambda}) - \frac{1}{3} \tilde{g}_\alpha^\lambda \tilde{g}_\beta^\tau$ , where  $\tilde{g}_{\alpha\beta} = -g_{\alpha\beta} + q^\alpha q^\beta / q^2$ . The coupling constant  $g_{D_0 D \pi} = 7.17$  GeV,  $g_{D_1(2420) D^* \pi} = 1.66$  GeV,  $g_{D_1(2430) D^* \pi} = 5.39$  GeV and  $g_{D_2 D^* \pi} = 5.11$  GeV $^{-2}$  can be obtained by the corresponding experimental width of  $\Gamma(D_0^*(2300) \rightarrow D\pi) \approx 229 \pm 16$  MeV [1],  $\Gamma(D_1(2420) \rightarrow D^*\pi) \approx 31.3 \pm 1.9$  MeV [1],  $\Gamma(D_1(2430) \rightarrow D^*\pi) \approx 314 \pm 29$  MeV [1] and  $\Gamma(D_2^*(2460) \rightarrow D^*\pi) \approx (47.3 \pm 0.8)/2.52$  MeV [1], respectively.

The total decay amplitude of  $\psi \rightarrow D^0 D^{*-} \pi^+$  reads

$$\begin{aligned} \mathcal{M} &= \mathcal{M}_{D_0} + e^{i\theta_1} \mathcal{M}_{D_1(2420)} + e^{i\theta_2} \mathcal{M}_{D_1(2430)} \\ &\quad + e^{i\theta_3} \mathcal{M}_{D_2(2460)}, \end{aligned} \quad (12)$$

where  $\theta_1, \theta_2, \theta_3$  are three unknown phase angles. Then, the three-body  $\pi^+ D^0 D^{*-}$  decay width can be calculated by

$$\Gamma_{3\text{-body}} = \int \frac{|\mathcal{M}|^2}{(2\pi)^5 16m_\psi^2} |q_2| |q_3| d\Omega_2 d\Omega_3 dm_{D^* \pi}, \quad (13)$$

where  $q_3^*$  and  $\Omega_3^*$  are the three momentum and solid angle of  $D^{*-}$  in the center of the  $D^{*-} \pi^+$  system mass frame, respectively. Based on the above formula, we firstly estimate the three-body decay width of  $\psi(4380) \rightarrow \pi^+ D^0 D^{*-}$ . The four related coupling constants  $g_{\psi DD_0} = 1.29$  GeV,  $g_{\psi DD_1(2420)} = 2.09$

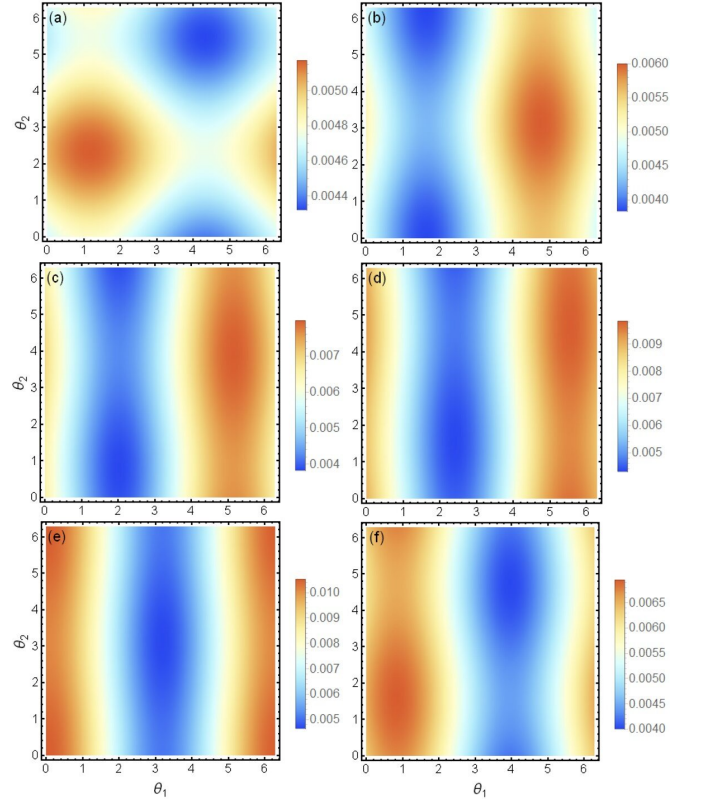


FIG. 2: The density plot of three-body decay width of  $\psi(4380) \rightarrow \pi^+ D^0 D^{*-}$  as a function of the  $\theta_1, \theta_2$  and  $\theta_3$ . Figure (a) to (f) corresponds to  $\theta_3 = 0, \pi/4, (2\pi)/4, (3\pi)/4, (5\pi)/4$  and  $(7\pi)/4$ , respectively. The width value is in unit of GeV.

GeV,  $g_{\psi DD_1(2430)} = 1.34$  GeV and  $g_{\psi DD_2} = 1.97$  GeV $^{-2}$  can be fixed by the corresponding theoretically estimated two-body widths listed in Ref. [21]. The width distribution plot of  $\psi(4380) \rightarrow \pi^+ D^0 D^{*-}$  over the full range  $[0 \sim 2\pi]$  of  $\theta_1, \theta_2$  and  $\theta_3$  is illustrated in Fig. 2. It can be seen that the three-body width is weakly dependent on  $\theta_2$  and its minimum 3.7 MeV appears near  $\theta_1 = \frac{\pi}{2} \sim \frac{3\pi}{4}$  and  $\theta_3 = \frac{\pi}{4} \sim \frac{\pi}{2}$  and maximum 10.9 MeV occurs around  $\theta_1 = 0$  and  $\theta_3 = \pi \sim \frac{5\pi}{4}$ . Considering the di-lepton width of  $\psi(4380) \rightarrow e^+ e^- = 260$  eV [21], we can estimate  $R_{\psi(4380)} = 12.0 \sim 35.8$  eV, which aligns with the fitted value of  $19.0 \pm 4.6$  eV listed in Table II. Similarly, we calculated  $\Gamma(\psi(4415) \rightarrow \pi^+ D^0 D^{*-}) = (0.35 \sim 1.9)$  MeV and  $\Gamma(\psi(4500) \rightarrow \pi^+ D^0 D^{*-}) = (1.5 \sim 5.5)$  MeV, which can be converted to be  $R_{\psi(4415)} = (2.4 \sim 13.5)$  eV and  $R_{\psi(4500)} = (3.3 \sim 12.3)$  eV, respectively, using the input values of  $\Gamma(\psi(4415) \rightarrow e^+ e^-) = 230$  eV [21, 41] and  $\Gamma(\psi(4500) \rightarrow e^+ e^-) = 113$  eV [21]. Remarkably, our theoretical results roughly confirm the dominant contribution of  $\psi(4380)$  in the  $e^+ e^- \rightarrow \pi^+ D^0 D^{*-}$  process through self-consistency, lending strong support to the proposed characterized energy level structure of higher vector charmonia. Moreover, it is worth noting that the theoretically predicted signal of  $\psi(4500) \rightarrow \pi^+ D^0 D^{*-}$  should exhibit a more pronounced line shape than the present data, which poses an intriguing

question for future precise experimental investigations.

*Summary.*— This letter aims to address the long-standing challenge of constructing the higher vector charmonium family above 4 GeV. By analyzing the open-charm process  $e^+e^- \rightarrow \pi^+ D^0 D^{*-}$  in detail, we reveal a remarkable agreement between the observed enhancement structures and the characterized energy level structure predicted by the unquenched potential model. The identified states, including  $\psi(4220)$ ,  $\psi(4380)$ ,  $\psi(4415)$ , and  $\psi(4500)$ , challenge conventional understanding and offer new insights into the dynamics of charm and anti-charm quarks in their formation. By overcoming multiple solution problems arising from resonance interference in the cross section analysis, we can further facilitate identification of characterized energy level structures of higher vector charmonia by comparing them with theoretical predictions of the three-body  $\pi^+ D^0 D^{*-}$  decay behaviors. By utilizing the effective decay amplitude, the calculated three-body decay behaviors of  $\psi \rightarrow \pi^+ D^0 D^{*-}$  sheds light on the properties of higher vector charmonia, particularly confirming the significant contribution of  $\psi(4380)$  in the  $e^+e^- \rightarrow \pi^+ D^0 D^{*-}$  process. Collectively, these findings provide strong evidence for the existence of the characterized energy level structure of higher vector charmonia. This work deepens our understanding of charmonium physics, emphasizing the need for precise experimental measurements of  $e^+e^- \rightarrow \pi^+ D^0 D^{*-}$  to further advance the study of charmonium spectroscopy above 4.0 GeV.

#### ACKNOWLEDGEMENTS

This work is supported by the China National Funds for Distinguished Young Scientists under Grant No. 11825503, the National Key Research and Development Program of China under Contract No. 2020YFA0406400, the 111 Project under Grant No. B20063, the National Natural Science Foundation of China under Grant Nos. 12247101 and 12047501, the Fundamental Research Funds for the Central Universities under Grant No. lzujbky-2023-stlt01, and the project for top-notch innovative talents of Gansu province. J.Z.W. is also supported by the National Postdoctoral Program for Innovative Talent.

\* Electronic address: [wangjzh2022@pku.edu.cn](mailto:wangjzh2022@pku.edu.cn)

† Electronic address: [xiangliu@lzu.edu.cn](mailto:xiangliu@lzu.edu.cn)

- [1] P. A. Zyla *et al.* [Particle Data Group], Review of Particle Physics, PTEP **2020**, no.8, 083C01 (2020).
- [2] H. X. Chen, W. Chen, X. Liu and S. L. Zhu, The hidden-charm pentaquark and tetraquark states, Phys. Rept. **639**, 1-121 (2016).
- [3] Y. R. Liu, H. X. Chen, W. Chen, X. Liu and S. L. Zhu, Pentaquark and Tetraquark states, Prog. Part. Nucl. Phys. **107**, 237-320 (2019).
- [4] H. X. Chen, W. Chen, X. Liu, Y. R. Liu and S. L. Zhu, An updated review of the new hadron states, Rept. Prog. Phys. **86**, no.2, 026201 (2023).
- [5] F. K. Guo, C. Hanhart, U. G. Meißner, Q. Wang, Q. Zhao and B. S. Zou, Hadronic molecules, Rev. Mod. Phys. **90**, no.1, 015004 (2018) [erratum: Rev. Mod. Phys. **94**, no.2, 029901 (2022)].
- [6] S. L. Olsen, T. Skwarnicki and D. Zieminska, Nonstandard heavy mesons and baryons: Experimental evidence, Rev. Mod. Phys. **90**, no.1, 015003 (2018).
- [7] N. Brambilla, S. Eidelman, C. Hanhart, A. Nefediev, C. P. Shen, C. E. Thomas, A. Vairo and C. Z. Yuan, The XYZ states: experimental and theoretical status and perspectives, Phys. Rept. **873**, 1-154 (2020).
- [8] J. J. Aubert *et al.* [E598], Experimental Observation of a Heavy Particle  $J$ , Phys. Rev. Lett. **33**, 1404-1406 (1974).
- [9] J. E. Augustin *et al.* [SLAC-SP-017], Discovery of a Narrow Resonance in  $e^+e^-$  Annihilation, Phys. Rev. Lett. **33**, 1406-1408 (1974).
- [10] E. Eichten, K. Gottfried, T. Kinoshita, J. B. Kogut, K. D. Lane and T. M. Yan, The Spectrum of Charmonium, Phys. Rev. Lett. **34**, 369-372 (1975) [erratum: Phys. Rev. Lett. **36**, 1276 (1976)].
- [11] E. Eichten, K. Gottfried, T. Kinoshita, K. D. Lane and T. M. Yan, Charmonium: The Model, Phys. Rev. D **17**, 3090 (1978) [erratum: Phys. Rev. D **21**, 313 (1980)].
- [12] S. Godfrey and N. Isgur, Mesons in a Relativized Quark Model with Chromodynamics, Phys. Rev. D **32**, 189-231 (1985).
- [13] L. P. He, D. Y. Chen, X. Liu and T. Matsuki, Prediction of a missing higher charmonium around 4.26 GeV in  $J/\psi$  family, Eur. Phys. J. C **74**, no.12, 3208 (2014).
- [14] Y. B. Dong, Y. W. Yu, Z. Y. Zhang and P. N. Shen, Leptonic decay of charmonium, Phys. Rev. D **49**, 1642-1644 (1994).
- [15] B. Q. Li and K. T. Chao, Higher Charmonia and  $X, Y, Z$  states with Screened Potential, Phys. Rev. D **79**, 094004 (2009).
- [16] M. Ablikim *et al.* [BESIII], Precise measurement of the  $e^+e^- \rightarrow \pi^+\pi^- J/\psi$  cross section at center-of-mass energies from 3.77 to 4.60 GeV, Phys. Rev. Lett. **118**, no.9, 092001 (2017).
- [17] M. Ablikim *et al.* [BESIII], Evidence of Two Resonant Structures in  $e^+e^- \rightarrow \pi^+\pi^- h_c$ , Phys. Rev. Lett. **118**, no.9, 092002 (2017).
- [18] M. Ablikim *et al.* [BESIII], Cross section measurements of  $e^+e^- \rightarrow \omega \chi_{c0}$  form  $\sqrt{s} = 4.178$  to 4.278 GeV, Phys. Rev. D **99**, no.9, 091103 (2019).
- [19] M. Ablikim *et al.* [BESIII], Measurement of  $e^+e^- \rightarrow \pi^+\pi^-\psi(3686)$  from 4.008 to 4.600 GeV and observation of a charged structure in the  $\pi^+\psi(3686)$  mass spectrum, Phys. Rev. D **96**, no.3, 032004 (2017) [erratum: Phys. Rev. D **99**, no.1, 019903 (2019)].
- [20] D. Y. Chen, X. Liu and T. Matsuki, Observation of  $e^+e^- \rightarrow \chi_{c0}\omega$  and missing higher charmonium  $\psi(4S)$ , Phys. Rev. D **91**, no.9, 094023 (2015).
- [21] J. Z. Wang, D. Y. Chen, X. Liu and T. Matsuki, Constructing  $J/\psi$  family with updated data of charmoniumlike  $Y$  states, Phys. Rev. D **99**, no.11, 114003 (2019).
- [22] J. Z. Wang and X. Liu, Confirming the existence of a new higher charmonium  $\psi(4500)$  by the newly released data of  $e^+e^- \rightarrow K^+K^- J/\psi$ , Phys. Rev. D **107**, no.5, 054016 (2023).
- [23] M. Ablikim *et al.* [BESIII], Evidence of a resonant structure in the  $e^+e^- \rightarrow \pi^+ D^0 D^{*-}$  cross section between 4.05 and 4.60 GeV, Phys. Rev. Lett. **122**, no.10, 102002 (2019).
- [24] M. Ablikim *et al.* [BESIII], Cross section measurements of the  $e^+e^- \rightarrow D^{*+} D^{*-}$  and  $e^+e^- \rightarrow D^{*+} D^-$  processes at center-of-mass energies from 4.085 to 4.600 GeV, JHEP **05**, 155 (2022).
- [25] M. Ablikim *et al.* [BESIII], Measurement of  $e^+e^- \rightarrow$

TABLE II: The fitted parameters of describing the cross section distribution of  $e^+e^- \rightarrow \pi^+D^0D^{*-}$  based on the scheme involving the characterized energy level structures of higher charmonia, where the  $\chi^2/d.o.f. = 0.74$ .

Parameters	$a_0$ ( $\text{GeV}^{-2}$ )	$g$ ( $\text{GeV}^{-3}$ )	$R_{\psi(4160)}$ (eV)	$R_{\psi(4220)}$ (eV)	$R_{\psi(4380)}$ (eV)	$R_{\psi(4415)}$ (eV)
Values	$0.445 \pm 0.025$	$34.5 \pm 18.1$	$0.726 \pm 0.527$	$2.70 \pm 0.63$	$19.0 \pm 4.6$	$2.34 \pm 1.23$
Parameters	$R_{\psi(4500)}$ (eV)	$\phi_{\psi(4160)}$ (rad)	$\phi_{\psi(4220)}$ (rad)	$\phi_{\psi(4380)}$ (rad)	$\phi_{\psi(4415)}$ (rad)	$\phi_{\psi(4500)}$ (rad)
Values	$1.60 \pm 0.42$	$1.97 \pm 0.65$	$2.07 \pm 0.15$	$1.44 \pm 0.16$	$6.04 \pm 0.24$	$5.76 \pm 0.31$

$\pi^+\pi^-D^+D^-$  cross sections at center-of-mass energies from 4.190 to 4.946 GeV, Phys. Rev. D **106**, no.5, 052012 (2022).

- [26] M. Ablikim *et al.* [BESIII], Observation of Three Charmoniumlike States with  $J^{PC} = 1^{--}$  in  $e^+e^- \rightarrow D^{*0}D^{*-}\pi^+$ , Phys. Rev. Lett. **130**, no.12, 121901 (2023).
- [27] [BESIII], Precise measurement of the  $e^+e^- \rightarrow D_s^{*+}D_s^{*-}$  cross sections at center-of-mass energies from threshold to 4.95 GeV, [arXiv:2305.10789 [hep-ex]].
- [28] E. van Beveren, C. Dullemond and T. A. Rijken, On the Influence of Hadronic Decay on the Properties of Hadrons, Z. Phys. C **19**, 275 (1983).
- [29] Y. S. Kalashnikova, Coupled-channel model for charmonium levels and an option for  $X(3872)$ , Phys. Rev. D **72**, 034010 (2005).
- [30] M. R. Pennington and D. J. Wilson, Decay channels and charmonium mass-shifts, Phys. Rev. D **76**, 077502 (2007).
- [31] B. Q. Li, C. Meng and K. T. Chao, Coupled-Channel and Screening Effects in Charmonium Spectrum, Phys. Rev. D **80**, 014012 (2009).
- [32] C. Z. Yuan, X. H. Mo and P. Wang, Multiple solutions in extracting physics information from experimental data, Int. J. Mod. Phys. A **25**, 5963-5972 (2010).
- [33] K. Zhu, X. H. Mo, C. Z. Yuan and P. Wang, A mathematical review on the multiple-solution problem, Int. J. Mod. Phys. A **26**, 4511-4520 (2011).
- [34] Y. Bai and D. Y. Chen, General mathematical analysis on multiple solutions of interfering resonances combinations, Phys. Rev. D **99**, no.7, 072007 (2019).
- [35] Knopp, K. (1996), "Weierstrass's Factor-Theorem", Theory of Functions, Part II, New York: Dover, pp. 1-7.
- [36] T. Barnes, S. Godfrey and E. S. Swanson, Higher charmonia, Phys. Rev. D **72**, 054026 (2005).
- [37] S. Godfrey and K. Moats, Bottomonium Mesons and Strategies for their Observation, Phys. Rev. D **92**, no.5, 054034 (2015).
- [38] J. Z. Wang, Z. F. Sun, X. Liu and T. Matsuki, Higher bottomonium zoo, Eur. Phys. J. C **78**, no.11, 915 (2018).
- [39] Q. T. Song, D. Y. Chen, X. Liu and T. Matsuki, Higher radial and orbital excitations in the charmed meson family, Phys. Rev. D **92**, no.7, 074011 (2015).
- [40] R. Casalbuoni, A. Deandrea, N. Di Bartolomeo, R. Gatto, F. Feruglio and G. Nardulli, Phenomenology of heavy meson chiral Lagrangians, Phys. Rept. **281**, 145-238 (1997).
- [41] M. Ablikim *et al.* [BES], Determination of the  $\psi(3770)$ ,  $\psi(4040)$ ,  $\psi(4160)$  and  $\psi(4415)$  resonance parameters, eConf **C070805**, 02 (2007).